Reducing under-sampling artifacts in 3D true-amplitude RTM angle gathers

Yilong Qin , Marcel Nauta and Scott Quiring, Acceleware Ltd.*

Summary

High resolution true-amplitude RTM Angle-Domain Common Image Gathers (ADCIGs), indexed by subsurface reflection and azimuth angles, can be used for:

- Evaluation of complex velocity models with multiple arrivals
- More reliable automatic picking of event curvature for tomographic inversion
- Angle-domain NMO de-stretch
- Azimuthal AVA analysis
- Azimuthal anisotropy analysis
- Angle-dependent subsurface illumination compensation
- Optimal adaptive stacking
- Multiple attenuation in subsalt area
- Impedance and velocity inversion
- Scattering-angle filtering for FWI
- Removal of RTM backscattered low-frequency noise.

In practice, the coarsely-sampled or irregularly-sampled shot and receiver locations on the surface leads to severe under-sampling artifacts in ADCIGs with small angle binning size. These under-sampling artifacts are worse for the shallow reflectors and small reflection angle in the case of 3D data.

In this paper, we first derive that the theoretical number of hitcount for each angle bin is given by the determinant of the Jacobian matrix of transforming subsurface angle to surface shot coordinates. Then we illustrate that the under-sampling artifacts are linearly proportional to the percentage deviation of actual hitcount number with respect to the theoretical hitcount number. At last, we propose using relative hitcount compensation to reduce the under-sampling artifacts for RTM 3D ADCIGs, and demonstrate its effectiveness on 3D synthetic.

Introduction

For complex velocity model with multiple arrivals, Angle-Domain Common Image Gathers (ADCIGs), indexed by subsurface angle, suffer less from migration artifacts than the Offset-Domain Common Image Gathers (ODCIGs) indexed by surface shot-receiver offset. The wave propagation in RTM carries more accurate amplitude in complex geology. Therefore, the 3D ADCIGs generated in RTM is more reliable for migration velocity update, angle-dependent illumination analysis and Amplitude Variation with Azimuth (AVAZ) analysis in the subsalt region. However, to increase the fidelity of these different applications, we need to generate amplitude-preserved high-resolution RTM 3D ADCIGs.

Calculation of 3D angle-domain CIGs is a mapping process from a 5D input space $(x_s, y_s; x_r, y_r; t)$ to a 5D image space $(x, y, z; \theta, \phi)$. The specular energy recorded in the regular acquisition geometry is irregularly sampled in the subsurface azimuth and opening angle domain. In the 3D case, the sampling rate of reflection angles $\Delta\theta$ and azimuth angle $\Delta\phi$ in the 3D ADCIGs is related to the shot spacing Δx_s and Δy_s at acquisition surface by (Bleistein et al., 2005; Zhang et al., 2007).

$$\Delta\theta\Delta\phi = \left|\frac{\partial(\theta,\phi)}{\partial(x_s,y_s)}\right| \Delta x_s \Delta y_s = \frac{\cos\alpha_{s0}}{v_{s0}} \frac{16\pi^2 A_s^2 v(x)}{\sin\theta} \Delta x_s \Delta y_s \quad (1)$$

Where v_{s0} is the wave speed at the shot points, and α_{s0} is the emergence angles of the ray from the image point to the shot. A_s is the amplitude from the source to the image point. $v(x)$ is the wave speed at image location. Assuming a constant velocity, this 3D angular sampling equation is simplified into

$$\Delta\theta\Delta\phi = \frac{\cos^3\theta}{z^2} \frac{1}{\sin\theta} \Delta x_s \Delta y_s \quad (2)$$

Where z is the reflector's depth. From equation 2, it can be seen that when mapping the regularly-sampled data acquired at surface to subsurface angle domain, the specular energy yields irregular distribution in the subsurface reflection/azimuth angle domain. The angular sampling rate of specular seismic events decreases with depth and reflection angle. For shallow events, the specular energy illuminates a wide range of reflection angles with a larger angle sampling increment at small reflection angles. As a result, the shallow events in 3D ADCIGs will have more under-sampling artifacts. The problem becomes more severe at smaller angles.

To attenuate these under-sampling artifacts, a natural choice is to interpolate the seismic data on the recording surface by using a 5D data regularization algorithm to create a dense shot spacing. However, interpolation onto a dense grid increases the number of shot gathers significantly, which will increase the computational cost for common-shot RTM (Tang et al., 2011). A simple solution is to smooth the angle gather using an adaptive smoothing length, but simple smoothing cannot solve the severe under-sampling issues and may harm the AVA response. Tang et al., (2013) have investigated this under-sampling issue in 3D RTM angle gathers and propose using plane-wave RTM with a number of different linear time delays.

In this paper, we first show that the under-sampling artifacts are a direct consequence of the relative deviation of the actual hitcount number from the corresponding theoretical hitcount number. Then, we propose to reduce the under-sampling artifacts by using relative hitcount compensation.

Theoretical hitcount number for true-amplitude 3D angle gather

The true-amplitude 3D ADCIGs can be obtained with the following angle-domain inversion formula (Zhang et al., 2007, 2014)

$$R(\mathbf{x};\theta,\phi) = \frac{16\pi^2 v(\mathbf{x})}{\Delta\theta\Delta\phi}\int\int \frac{i\omega}{\sin\theta}\frac{\cos\alpha_{s0}\cos\alpha_{r0}}{v_{s0}v_{r0}} A_s A_r e^{i\omega(\tau_s+\tau_r)} D(\mathbf{x}_s;\mathbf{x}_r,\omega)\,d\omega\,d^2\mathbf{x}_s\,d^2\mathbf{x}_r \quad (3)$$

Where $R(\mathbf{x};\theta,\phi)$ gives the angle- and azimuth-dependent reflectivity with correct migration velocity and fine enough source and receiver spacing. θ is the reflection angle and ϕ is the azimuth angle. x, x_s and x_r represent image location, source location and receiver location respectively. $v(\mathbf{x})$ is the wave speed at the image point. v_{s0} and v_{r0} are the wave speeds at the shot and receiver points, and α_{s0} and α_{r0} are the emergence angles of the ray from the shot and receiver points to the image point, respectively. A_s (A_r) and $\tau_s(\tau_r)$ are the amplitude and traveltime from source (receiver) to image point. $D(x_s;x_r,\omega)$ is the observed seismic data at the acquisition surface. The term $1/\sin\theta$ is needed to compensate for the diminishing area when the reflection angle tends to 0^o. The 3D angle-domain inversion formula has a singularity at $\theta = 0^o$, which causes difficulty in obtaining accurate amplitudes around the zero reflection angle. Equation 3 shows that true-amplitude, angle-domain inversion require a cross-correlation imaging condition, instead of deconvolution imaging condition as used in true-amplitude common-shot inversion.

Equation 3 can be re-written as (Bleistein et al., 2005)

$$R(\mathbf{x};\theta,\phi) = \frac{1}{\Delta\theta\Delta\phi}\int R_s(\mathbf{x};\mathbf{x}_s)\left|\frac{\partial(\mathbf{x}_s)}{\partial(\theta,\phi)}\right|^{-1} d^2\mathbf{x}_s \quad (4)$$

where $R_s(\boldsymbol{x};\mathbf{x}_s) = \int i\omega \frac{cos\alpha_{r0}}{v_{r0}}\frac{A_r}{A_s} e^{i\omega(\tau_s+\tau_r)} D(\mathbf{x}_s;\mathbf{x}_r,\omega)\,d\omega\,d^2\mathbf{x}_s\,d^2\mathbf{x}_r$ is the 3D common-shot inversion formula which gives the true-amplitude common-shot image. $\left|\frac{\partial(\mathbf{x}_s)}{\partial(\theta,\phi)}\right|^{-1} = \frac{\cos\alpha_{s0}}{v_{s0}}\frac{16\pi^2 A_s^2 v(\mathbf{x})}{\sin\theta}$ is the determinant of the Jacobian matrix of transforming surface variables $\mathbf{x}_s$ to subsurface angle variables (θ,ϕ). Equation 4 shows that the true-amplitude 3D RTM ADCIGs can also be obtained as the weighted summation of true-amplitude 3D RTM shot images, although equation 3 is often used in the actual implementation (Zhang et al., 2007). The term $\left|\frac{\partial(\mathbf{x}_s)}{\partial(\theta,\phi)}\right|^{-1}$ acts as the weighting coefficient for the summation of the true-amplitude common-shot image. From equation 4, we infer that in order to produce the true-amplitude 3D angle gather, the actual number of the hitcount for each pair of azimuth and reflection angle bins should be linearly proportional to the Jacobian of transforming subsurface angle variables (θ,ϕ) to surface variables $\mathbf{x}_s$, i.e.,

$$\left|\frac{\partial(\mathbf{x}_s)}{\partial(\theta,\phi)}\right| = \frac{v_{s0}}{cos\alpha_{s0}}\frac{sin\theta}{16\pi^2 A_s^2 v(\boldsymbol{x})} \quad (5)$$

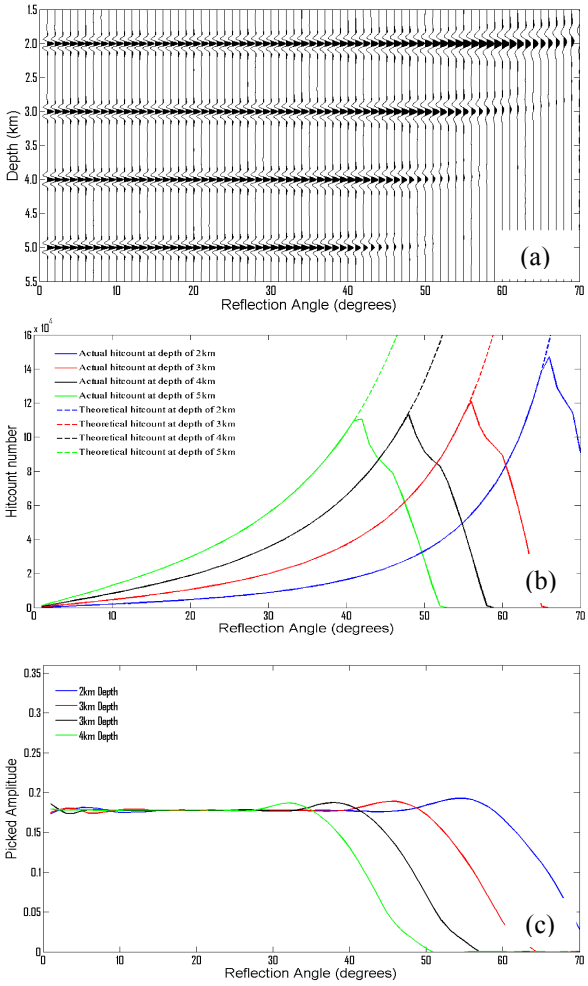

Figure 1. 3D true-amplitude angle gather obtained using shot spacing of 2.5m by 2.5m. (a) RTM angle gather with reflection angle bin of 1 degree. (b) Comparison of actual hitcount number (solid line) with theoretical hitcount

number (dashed line) for each angle bin at different depths. (c) The AVA curves picked along the 4 reflectors.

To confirm this analysis, we use a 3D synthetic example to compare the actual number of specular hitcount with the theoretical number of hitcount as given in equation 5. To generate a 3D synthetic gather, we model four flat density-contrast reflectors at depths of 2.0, 3.0, 4.0 and 5.0 km in a constant velocity medium of 3000m/s. These 4 reflectors have the same theoretical angle-independent reflectivity. The input synthetic shot gather is generated by assuming the amplitudes of recorded reflected events are only affected by geometrical spreading. The receivers are located in a dense grid at 8km maximum offset in the inline and crossline directions. The source is at the center of receiver spread and a Ricker wavelet with a 10Hz peak frequency is used as source wavelet. We use RTM to generate 3D ADCIGs.

Figure 1a shows the ADCIGs with reflection angle bin of 1 degree for an azimuth range of $[0\ 60^0]$ by using a shot interval of 2.5m by 2.5m. From Fig. 1b, we can observe that with extremely small shot spacing, the actual hitcount number for each angle bin matches perfectly with the theoretical hitcount number, as given in equation 5. We can note that the hitcount number increases exponentially with reflection angle and reflector depth. Fig. 1c shows that the picked amplitude along the 4 reflectors is almost the same as the theoretical AVA curve, which confirms that equation 3 produces 3D true-amplitude ADCIGs when the shot spacing is small enough to eliminate under-sampling artifacts. In Figure 1c, the small amplitude oscillation at near angles is because the recorded reflection on the shot gather has a large curvature near zero offset.

Reducing the under-sampling artifacts by relative hitcount compensation

The correlation-type angle-domain inversion formula in equation 3 involves an integral process over shots. Therefore it requires sufficiently dense shots, such that the discrete sum over the shots is a reasonable approximation of the integral over the shots. However, for most current 3D surveys, the coarsely sampled shot and receiver locations on the surface will lead to severe subsurface angular under-sampling artifacts. These artifacts are worse for shallow seismic events and 3D ADCIGs with small reflection angle bin sizes, whereas the small angle binning size is needed for reliable residual curvature picking (Tang et al., 2011) and high-resolution migration velocity analysis using angle gathers.

To illustrate the under-sampling artifacts in the 3D RTM ADCIGs, we use the same 3D model as used in Figure 1, but increase the shot spacing to 80m by 80m. Figure 2 shows the ADCIGs with a reflection angle bin of 1 degree for the azimuth range of $[0\ 60^0]$ generated using this large shot spacing and the corresponding hitcount analysis. The picked AVA curves are shown in Figure 2b. By comparing Figure 2b and 1c, it is obvious to see that the under-sampling artifacts are caused by large shot spacing and that they are worse for shallow events with small reflection angles. Fig. 2d shows the percentage error of actual hitcount with respect to the theoretical hitcount. By comparing Fig. 2b and 2c, it can be seen that the amplitude error caused by under-sampling artifacts has almost the same variation as the percentage error of actual hitcount. This illustrates that the under-sampling artifacts in ADCIGs is a direct consequence of the deviation of actual hitcount from the theoretical number of hitcount.

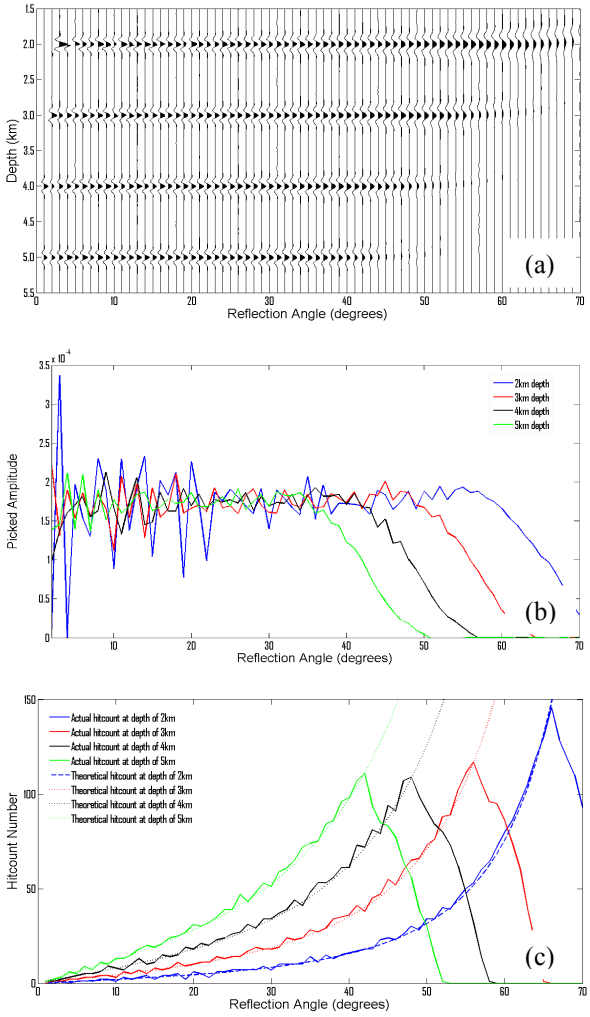

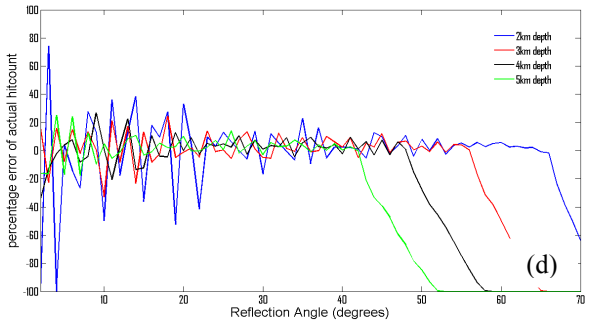

Figure 2. 3D true-amplitude angle gather obtained using shot spacing of 80mx80m. (a) RTM angle gather with reflection angle bin of 1 degree. (b) The AVA curves picked along the 4 reflectors in (a). (b) Comparison of actual hitcount number with the theoretical hitcount number for each angle bin at different depths. (c) Percentage error of actual hitcount number with respect to theoretical hitcount number. The same model used in Figure 1 is used here.

From the analysis above, it is straightforward to propose using relative hitcount compensation to remove the under-sampling artifacts in RTM ADCIGs. This relative hitcount compensation aims to compensate the inconsistency between actual hitcount number and theoretical hitcount number for each angle bin, instead of normalizing the amplitude by the actual hitcount number. Fig. 3a shows the corresponding ADCIGs after applying the relative hitcount compensation. It can be seen that after relative hitcount compensation, the ADCIGs look very similar to the results obtained by using a small spacing as shown in Fig. 1a. To illustrate the effectiveness of our method, we compare the angle traces before and after the relative hitcount compensation, as shown in Fig. 3b. It can be seen that the waveform is well recovered at the shallow imaged reflector and the high-frequency artifact caused by the under-sampling issue is removed.

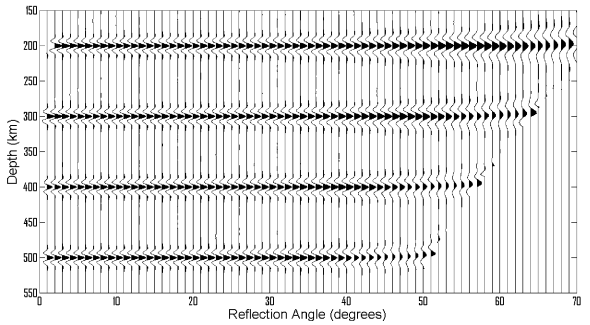

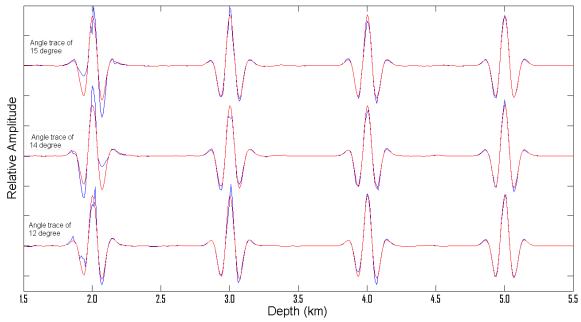

Figure 3. (a) 3D ADCIGs after applying the relative hitcount compensation to the result in Fig. 2a. (b) Comparison of angle traces from before (blue) and after (red) relative hitcount compensation. It can be seen that the under-sampling artifacts in near angles are completely removed for this example.

Conclusions and discussion

By analyzing the correlation-type true-amplitude angle-domain inversion formula, we demonstrate that the theoretical hitcount number for each azimuth/angle bin in ADCIGs is directly proportional to the Jacobian of transforming subsurface angular variables to surface source coordinate. Our 3D synthetic example shows that the under-sampling artifacts are a direct consequence of the deviation of actual specular hitcount number from the theoretical hitcount number. To reduce the under-sampling artifacts, we propose to weight each of the samples in ADCIGs by the ratio of theoretical number of hitcount vs actual specular hitcount number. The synthetic examples demonstrate the effectiveness of the relative hitcount compensation in reducing the under-sampling artifacts.

Our relative hitcount compensation scheme is also applicable to 2D/3D Kirchhoff, Beam or wave-equation migration angle gathers. One of the key steps is to calculate the actual specular hitcount number for each azimuth/angle bin for a given acquisition geometry and velocity model. We would also mention that the direct stack of the true-amplitude angle gathers doesn't guarantee that a true-amplitude stack image will be produced, since the range of valid illumination angles usually varies with depth and the AVA effect is not corrected.

Acknowledgements

The authors thank Acceleware Ltd. for permission to publish this work. We also thank Yoichi Yoshida and Stanley Tsang for the helpful discussions.

EDITED REFERENCES

Note: This reference list is a copyedited version of the reference list submitted by the author. Reference lists for the 2016 SEG Technical Program Expanded Abstracts have been copyedited so that references provided with the online metadata for each paper will achieve a high degree of linking to cited sources that appear on the Web.

REFERENCES

Bleistein, N., Y. Zhang, S. Xu, G. Zhang, and S. H. Gray, 2005, Migration/inversion: Think image point coordinates, process in acquisition surface coordinates: Inverse Problems, **21**, 1715–1744, http://dx.doi.org/10.1088/0266-5611/21/5/013.

Tang, B., S. Xu, and Y. Zhang, 2011, Aliasing in RTM 3D angle gathers: 81st Annual International Meeting, SEG, Expanded Abstracts, 3310–3314, http://dx.doi.org/10.1190/1.3627885.

Tang, B., S. Xu, and Y. Zhang, 2013, 3D angle gathers with plane-wave reverse-time migration: Geophysics, **78**, no. 2, S117–S123, http://dx.doi.org/10.1190/GEO2012-0313.1.

Zhang, Y., A. Ratcliffe, G. Roberts, and, L. Duan, 2014, Amplitude-preserving reverse time migration: From reflectivity to velocity and impedance inversion: Geophysics, **79**, no. 6, S271–S283, http://dx.doi.org/10.1190/GEO2013-0460.1.

Zhang, Y., S. Xu, N. Bleistein, and G. Zhang, 2007, True amplitude angle domain common image gathers from one-way wave equation migrations: Geophysics, **72**, no. 1, S49– S58, http://dx.doi.org/10.1190/1.2399371.